

Formation of Palladium Nanoclusters on Y-Zeolite via a Sonochemical Process and Conventional Methods

Kenji Okitsu,* Akihiko Yue, Shuji Tanabe,* Hiroshige Matsumoto

Faculty of Engineering, Nagasaki University, 1-14 Bunkyo-machi, Nagasaki 852-8521

(Received July 2, 2001)

The preparation of Pd clusters was investigated by the sonochemical reduction of $[Pd(NH_3)_4]^{2+}$ complexes on Y-zeolite in an aqueous solution at 20 °C. Through measurements of the UV–vis and X-ray photoelectron spectra, $[Pd(NH_3)_4]^{2+}$ was found to be reduced by radicals formed from 2-propanol sonolysis to yield zero-valent Pd. It was confirmed that the binding energy of the Pd 3d core level on the Y-zeolite was shifted to a higher value in comparison with that of Pd bulk metal. The formation of Pd metal, however, could not be observed by TEM and EXAFS measurements, implying the formation of ultrafine Pd clusters. On the other hand, the results of XPS analyses for several standard Pd clusters of ca. 1nm prepared by the conventional thermal treatment indicated that the peak values of the Pd core level increased with decreasing particle size. The maximum difference in binding energy between these samples was 0.6 eV at the Pd $3d_{5/2}$ core level. This phenomenon was suggested to be attributed to a quantum size effect corresponding to a splitting of the band structure. In comparison with standard samples, the size of sonochemically formed Pd clusters was roughly estimated to be less than 1 nm and composed of several dozen Pd atoms.

Small metal clusters have been found to show unique properties which are completely different from that in their bulk state. According to the quantum size effect, for example, it is well-known that a degenerate band structure is split as the size of the metal particles decreases, resulting in an increase in the band gap and a decrease in the electrical conductivity.[1] Changes in the melting point,[2] specific heat,[3] magnetism,[4] and catalytic activity[5,6] have also been reported in recent years. Metal clusters having such special physicochemical properties are, therefore, expected to be new materials which are quite different from the bulk state. Thus, the preparation and application of metal clusters as functional materials, and theories based on the experimental results are being actively pursued at the present time.

We have been investigating the reactivities of active radicals formed from cavitation bubbles with extremely high temperatures, which are generated by high-power ultrasonic irradiation, and have reported that reduction by radicals could be applied for preparing various noble metal nanoparticles, such as Pd, Au and Pt.[7–11] The cavitation is, in general, comprised of the formation, growth and collapse of bubbles in a liquid. When the cavitation bubbles are violently collapsing, the insides of the bubbles reach several thousand degrees and several hundred atmospheres, which are locally generated in a bulk solution and rapidly cooled to ambient temperature in excess of 10^{10} K/s.[12] The application of these extreme and unique conditions has focused on the preparation of new nanostructured materials, including catalytic, magnetic and semiconductive materials,[13] but there are few reports on the preparation of ultrafine metallic clusters with the quantum size effect. Several methods for preparing supported metallic clusters materials have so far been reported; i.e., chemical reduction with such strong reductants as hydrated electrons and $NaBH_4$ in solution,[14] and a metal evaporation technique in a high vacuum system.[15] Moreover, it was also reported[16,17] that small metal clusters could be prepared by consecutive oxidation-reduction treatments in a zeolite matrix with regularly ordered pore structures in the angstrom range, in which the rigid pore plays a role as a template to prevent metal aggregation under mild conditions.

In the present study, the development of a new application of ultrasound in the preparation of ultrafine Pd metal clusters was investigated by the sonochemical reduction of ion-exchanged $[Pd(NH_3)_4]^{2+}$ on Y-zeolite in an aqueous solution. Although the chemical effects of cavitation are generally characterized as a high-temperature reaction system, the reactions proceeding in a bulk solution apart from the hot cavities could be regarded as a low-temperature system. Because the reduction of metal ions with reducing radicals occurs in bulk solution,[7–11] the formation of metal clusters would be expected to occur under such a low temperature condition. In addition, the zeolite pore matrix acts as a template to prepare Pd clusters. At first, the reduction mechanism of the $[Pd(NH_3)_4]^{2+}$ ions both in a homogeneous and heterogeneous solution is discussed. For a comparison, several kinds of Pd clusters were prepared by consecutive oxidation–reduction processes in a conventional gas-phase reaction system. Characterization of the prepared materials was carried out mainly by extended X-ray absorption fine-structure (EXAFS) and X-ray photoelectron spectroscopy (XPS).

Experimental

Reagents. The original sample of Y-zeolite (LZY-54 type: $Na_{56}(AlO_2)_{56}(SiO_2)_{136}$) was purchased from Union Showa. Tetraamminepalladium(II) dichloride was obtained from Mitsuwa Chemicals. Reagent-grade NaCl, NaI, 2-propanol, and Pd black

were purchased from Wako Pure Chemical Industries. These chemicals were used without further purification. Argon and oxygen of 99.99% purity from Japan Air Liquid and hydrogen of 99.99999% purity from Nippon Sanso were used in the present experiments.

Preparation of $Pd(NH_3)_4$–Zeolite. The ion-exchange of Na–Y-zeolite with $[Pd(NH_3)_4]^{2+}$ ions was performed by a conventional method; i.e., Y-Zeolite washed with distilled water was suspended in a NaCl solution (0.1 M) and vigorously stirred at 70 °C for 12 h to obtain a thoroughly ion-exchanged Na^+-type zeolite sample. The sample was washed with distilled water again and then dried in an oven overnight. To an aqueous suspension of the sample, an aqueous solution of $[Pd(NH_3)_4]Cl_2$ was slowly added to yield 5–7wt% of Pd loaded on the zeolite. This ion-exchange with $[Pd(NH_3)_4]^{2+}$ was carried out at 50 °C for 12 h with stirring. The sample was then filtered and washed sufficiently with distilled water until no chloride ion could be detected, which was confirmed by the addition of silver ions. The $Pd(NH_3)_4$–zeolite obtained was dried at 50 °C in an oven for one day.

Procedure of Ultrasonic Irradiation. Ultrasonic irradiation was carried out at 20 °C in a water bath using an ultrasonic generator (Kaijo 4021, 200 kHz, 6 W/cm^2) with a 65 mmϕ barium titanate oscillator. Details of the irradiation setup are shown in a previous report.[9] The $Pd(NH_3)_4$–zeolite powders were added into water in the reaction vessel (65 mL, 29 mg), and then dispersed with an ultrasonic cleaner at 28 kHz for 1 min. The solution was bubbled with argon for 30 min to remove air, and then 0.486 mL of 2-propanol was injected into the solution (corresponding to 100 mM) using a micro-syringe through the septum. Ultrasonic irradiation was carried out for 2 h, in which a purge with argon and the addition of 2-propanol were done every 30 min during irradiation. The vessel was closed to the atmosphere during the course of irradiation. In order to confirm the sonochemical reduction of $[Pd(NH_3)_4]^{2+}$, ultrasonic irradiation of a homogeneous aqueous solution of $[Pd(NH_3)_4]^{2+}$ (65 mL, 0.2 mM) was carried out in argon atmosphere, where 0.486 mL of 2-propanol was injected into the solution through the septum just before irradiation. The irradiated solution was sampled through the septum by a glass syringe and then analyzed.

Colorimetric Analysis. The UV-vis absorption spectra of the irradiated solutions were measured by a spectrophotometer (Shimadzu UV-2100). The concentration of $[Pd(NH_3)_4]^{2+}$ was determined by an improved colorimetric method using NaI,[10] i. e., the absorption peak of $[PdI_4]^{2-}$ corresponding to $[Pd(NH_3)_4]^{2+}$, which was formed in a ligand-exchange reaction between NH_3 and I^-, was clearly observed at 408 nm by the addition of a saturated NaI solution into the sample. At the same time, the aggregation of colloidal Pd occurred, so that it could be removed easily by filtration. This colorimetric analysis was carried out for a solution filtered through a membrane filter with a pore size of 0.2 μm to avoid any spectrophotometrical interference of formed Pd aggregates after the addition of the NaI solution. Because the ligand-exchange reaction between NH_3 and I^- was very slow, the absorption spectra were determined 12 h after adding of the NaI solution. A calibration was also carried out with a known concentration of $[Pd(NH_3)_4]^{2+}$ solution.

Preparation of Pd–Zeolite via Conventional Thermal Treatments. For a comparison, three types of Pd–zeolite were prepared by the following methods:[16] (1) R Treatment: the ion-exchanged $Pd(NH_3)_4$–zeolite of 16–32 mesh was placed in a conventional flow reaction system with a quartz tube, and then reduced with hydrogen at 400 °C for 2 h [Pd–zeolite (R)]. (2) O-R1 Treatment: the ion-exchanged $Pd(NH_3)_4$–zeolite of 16–32 mesh was oxidized initially with oxygen 150 °C for 2 h and then reduced with hydrogen at 400 °C for 2 h [Pd–zeolite (O-R1)]. (3) O-R2 Treatment: the Pd–zeolite (O-R1) was reoxidized with oxygen at 400 °C for 2 h and then reduced with hydrogen at 50 °C for 2 h [Pd–zeolite (O-R2)]. These treatments were carried out with the reactant gas at a flow rate of 100 mL/min and a heating rate of 5 °C/min.

Characterization of the Pd–Zeolite. The specimens for transmission electron microscopy (TEM) analysis were prepared as follows. A sonochemically prepared sample was added to a small amount of water and then dispersed by an ultrasonic cleaner for 1min. This suspension was dropped onto a Cu grid coated with collodion film and dried in a vacuum. The TEM observations were carried out with electron microscopes (JEOL JEM 2010-UHR operated at 200 kV and JEM-100S operated at 100 kV). The X-ray photoelectron spectra of the Pd-zeolite samples were measured by a spectrometer (Shimadzu ESCA-850). The Pd-zeolite samples were pressed into thin wafers (ca. 10 mg/cm^2) and placed on a sample holder using an adhesive carbon tape. An X-ray source with a magnesium target was operated at 8 kV and 30 mA under below 2×10^{-5} Torr (1 Torr $\approx$ 133.322 Pa). The binding energy was corrected by simultaneously measuring the C 1s binding energy. After a charge-up correction using the value of the binding energy of the C 1s level, the binding energy of the Si 2p and Al 2p levels was in good accord with that of the literature. In the present study, the average of the binding energy of C 1s and its standard deviation was 287.65 eV and 0.078 eV, respectively, which was evaluated based on the values of six different samples. The EXAFS measurements were performed by an in-situ system, described elsewhere.[18] Basically, it consists of a rotating anode X-ray generator (Rigaku Ru-200), a spectrometer with a bent silicon (220) crystal by Johansson cut, ion chambers, slits, and counting electronics by a computer through a CAMAC bus. The X-ray source with a gold target was operated at 40 kV and 360 mA. Pd-zeolite samples were pressed into thin wafers and measured by in-situ EXAFS under each condition of the O-R treatments. The detailed method used for the data analysis has also been described elsewhere.[18]

Results and Discussion

Ultrasonic Irradiation of a $[Pd(NH_3)_4]^{2+}$ Solution. A homogeneous aqueous solution of $[Pd(NH_3)_4]Cl_2$ (0.2 mM) was transparent, and the color hardly changed upon ultrasonic irradiation, even in an argon atmosphere. In the presence of 2-propanol, on the other hand, the solution gradually turned to a dark-brown color during irradiation. Figure 1 shows the absorption spectra of the solution during the course of irradiation. A broad absorption band from the visible to the ultraviolet region clearly emerged upon irradiation, and rapidly increased with increasing irradiation time. In addition, a surface plasmon peak attributed to ultrafine particles of Pd metal (λ = 225 nm)[19] was also observed. Although the peak position of the Pd surface plasmon has been known to be located in the far-UV, theoretically,[19] it was very difficult to confirm the peak experimentally because it would be easily hidden when some coexisting ions and stabilizers, such as a surfactant, are present in the colloidal solution. Taking into account coexisting solutes in the present experiment,[20] the absorption spectra were corrected, as shown in Fig. 2. The absorption spectra of the surface plasmon corresponding to metallic Pd particles were

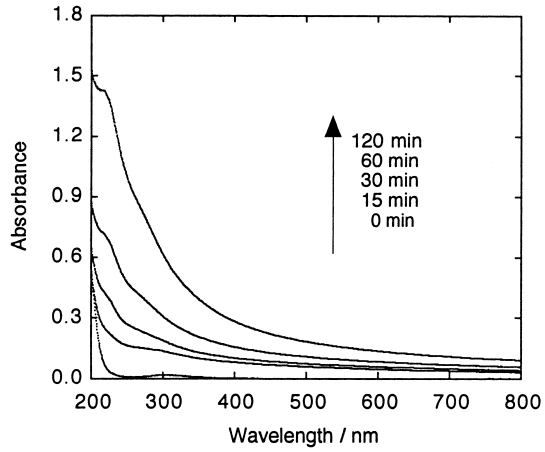

Fig. 1. Changes in the absorption spectra of $[Pd(NH_3)_4]Cl_2$ solution in the presence of 2-propanol during ultrasonic irradiation. Conditions; 0.2 mM $[Pd(NH_3)_4]Cl_2$, 100 mM 2-propanol; Ar atmosphere; Cell length, 0.5 cm.

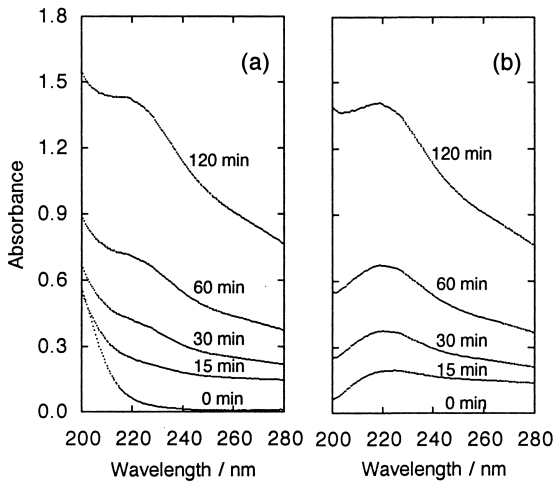

Fig. 2. Absorption spectra of sonochemically formed Pd colloid before (a) and after (b) the corrections. Conditions; same as shown in Fig. 1.

clearly observed. The formed Pd particles were extremely stable in the colloidal state for more than six months, even in the absence of stabilizers. Figure 3 shows a transmission electron micrograph of the Pd nanoparticles formed by ultrasonic irradiation. It was observed that spherical Pd particles were formed. The average size of the particles was about 20–30 nm with a relatively narrow distribution, although no stabilizer existed in the solution.

It has been reported that there are three different regions in the aqueous sonochemical process: 1) The inside of the collapsing cavitation bubbles where several thousand degrees and several hundred atmospheres are produced. Here, water vapor is pyrolyzed into H atoms and OH radicals. 2) The interfacial region between the cavitation bubbles and the bulk solution where the temperature is lower than that inside the cavitation bubbles, but still high enough for thermal decomposition of solutes to occur. 3) The bulk solution at ambient temperature where the reactions of solute molecules with OH radicals or H

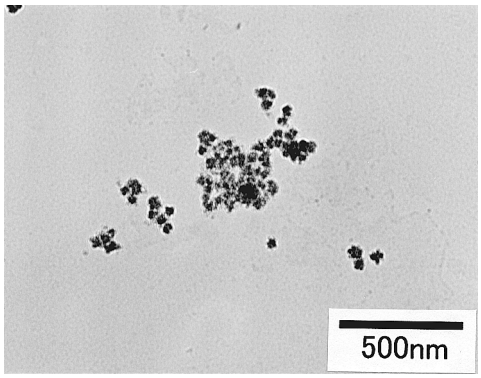

Fig. 3. TEM photograph of the Pd particles formed from sonochemical reduction of $[Pd(NH_3)_4]^{2+}$ in the presence of 2-propanol.

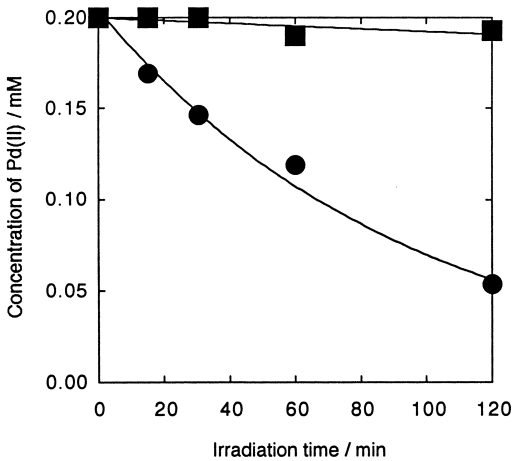

Fig. 4. Changes in the concentration of $[Pd(NH_3)_4]^{2+}$ during ultrasonic irradiation in the absence (■) and presence (●) of 100 mM 2-propanol.

atoms, which escaped from the interfacial region, take place. In previous reports, we have proposed that locally generated cavitation bubbles initiate the following chemical reactions:

$$H_2O \rightarrow {}^{\bullet}OH + {}^{\bullet}H \quad (1)$$

$$(CH_3)_2CHOH + {}^{\bullet}OH({}^{\bullet}H) \rightarrow (CH_3)_2{}^{\bullet}COH + H_2O(H_2) \quad (2)$$

$$(CH_3)_2CHOH \rightarrow \text{pyrolysis radicals} \quad (3)$$

$$Pd(NH_3)_4{}^{2+} + \text{reducing radicals} \rightarrow \rightarrow Pd \quad (4)$$

where Eqs. 1 to 3 indicate the sonochemical formation of reducing radicals, such as H atoms, 1-hydroxy-1-methylethyl radicals and pyrolysis radicals,[9,10] respectively, and Eq. 4 indicates the reduction of $[Pd(NH_3)_4]^{2+}$ by such reducing radicals. In fact, it has been reported that 1-hydroxy-1-methylethyl radicals, as shown in Eq. 2, are also formed by irradiation with ultraviolet[21] and γ-rays[22] of an aqueous solution of 2-propanol, whose radicals are well-known to act as a high-potential reducing agent.

Figure 4 shows the change in the concentration of $[Pd(NH_3)_4]^{2+}$ ions during ultrasonic irradiation in the absence

and presence of 2-propanol. In the presence of 2-propanol, the concentration of these ions rapidly decreased with an increase in the irradiation time, and the initial rate of reduction was estimated to be 2.1 μM/min at an initial $[Pd(NH_3)_4]^{2+}$ concentration of 0.2 mM. In comparison with the sonochemical reduction of $[PdCl_4]^{2-}$ ions,[10] the rate of $[Pd(NH_3)_4]^{2+}$ reduction was found to be extremely slow. Misik and Riesz[23] have identified by a spin trapping ESR method that various types of radicals are formed in the sonolysis of organic compounds. In the sonolysis of 2-propanol, pyrolysis radicals, such as CH_3 and CH_3CHCH_3 radicals, were also reported to be formed [corresponding to Eq. 3]. In the present study, we consider that 1-hydroxy-1-methylethyl radicals formed from the abstraction reaction,[24] as represented in Eq. 2, are one of the most important radicals for reducing the $[Pd(NH_3)_4]^{2+}$ ions. The reasons are that the $[Pd(NH_3)_4]^{2+}$ reduction by H atoms formed in water sonolysis did not take place (Fig. 4) and that the rate of $[Pd(NH_3)_4]^{2+}$ reduction was extremely slow compared to that of the formation of pyrolysis radicals, which could be roughly estimated from the sonochemical reduction of $[PdCl_4]^{2-}$ ions.[10] It was also found that the direct reduction of $[Pd(NH_3)_4]^{2+}$ with water did not take place in the interfacial region, because the reduction did not occur in the absence of 2-propanol. This result was supported by a property of $[Pd(NH_3)_4]^{2+}$ ions based on the Gibbs adsorption equation: because $[Pd(NH_3)_4]^{2+}$ is a hydrophilic compound, such a molecule cannot accumulate at the interface of the bubbles. These obtained results suggest that the reduction of $[Pd(NH_3)_4]^{2+}$ with a reducing radical proceeds in the bulk solution maintained at ambient temperatures.

Preparation and Characterization of the Pd–Zeolite. An aqueous suspension of the $Pd(NH_3)_4$-zeolite containing 100 mM 2-propanol was irradiated with high-power ultrasound. The color of the $Pd(NH_3)_4$–zeolite powders gradually changed from white to dark gray during irradiation. Figure 5 shows the XPS spectra for the Pd 3d core level of the zeolite sample before and after irradiation. Before irradiation, the binding energy corresponding to divalent Pd ions (Pd(II)) was clearly confirmed (Pd $3d_{3/2}$ 344.1 eV and Pd $3d_{5/2}$ 339.0 eV). The intensity of both peaks decreased upon ultrasonic irradiation, and new peaks were observed at 342.6 eV and 336.9 eV. These chemical shifts to lower energy by ca. 2 eV support the progress of $[Pd(NH_3)_4]^{2+}$ reduction into zerovalent Pd (Pd(0)) upon irradiation. On the other hand, the reduction did not proceed in the absence of 2-propanol, similar to the homogeneous solution mentioned above, indicating that the reduction of $[Pd(NH_3)_4]^{2+}$ in a heterogeneous solution also proceeded with reducing radicals and no thermal reduction near the cavitation hot bubbles occurred. Therefore, the reduction of $[Pd(NH_3)_4]^{2+}$ on the zeolite occurred at an ambient temperature of around 20 °C. In the present 200 kHz sonication system, because the size of the resonance bubbles is considerably smaller than those formed by a horn-type ultrasonic oscillator at 20–40 kHz frequency, the lifetime of the bubbles is considered to be relatively short.[25] Thus, we speculate that the mechanical effects and direct thermal effects generated from collapsing bubbles would be small. Furthermore, the formation of cavitation bubbles is difficult to take place in a zeolite pore with an effective diameter of less than 1.2nm. XPS depth analyses of the samples were carried out by argon sputtering. These results indicated that the $[Pd(NH_3)_4]^{2+}$ ions in the zeolite pore were not sufficiently reduced, even in the presence of 2-propanol. Presumably, the reducing radicals formed from 2-propanol sonolysis could not easily diffuse into the zeolite micro-pore or the radicals would vanish due to recombination reactions and quenching with the walls.

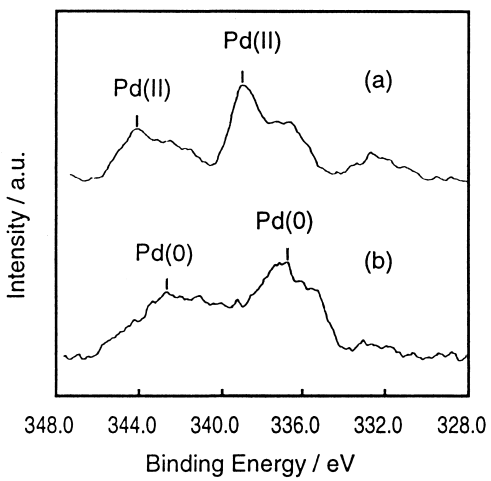

Fig. 5. X-ray photoelectron spectra of Pd 3d core level before (a) and after (b) the irradiation in the presence of 2-propanol.

Charge-up phenomena in the XPS measurements were observed for all elements (Al, Si, O, Pd and C) because of the insulating property of the zeolite skeleton. In addition, a differential charging phenomenon was recognized in the Pd analysis as follows: the binding energy corresponding to the Pd 3d core level on zeolite was still shifted to a higher energy by ca. 0.9 eV relative to that of bulk Pd, even if a charge-up correction was performed. Such differential charging phenomena are often observed when fine metal particles with electronic conductivity are supported on a metal oxide insulator. The chemical shift of the observed binding energy would be considered to be due to a change in the interaction of electron transfer etc. Recently, Bukhtiyarov et al.[26] reported that the binding energy of the Ag $3d_{5/2}$ core level in Ag supported on α-Al_2O_3 shifted to a lower energy relative to that of the bulk Ag state. In the Pd species prepared by sonochemical reduction, it was also proved that the binding energy of zero-valent Pd was much more distinctly shifted to higher values compared to that of the bulk state of metallic Pd. This phenomenon is discussed in detail in a later section.

Figure 6 shows a TEM photograph of the Pd-zeolite after ultrasonic irradiation in the presence of 2-propanol. In the TEM picture, regularly ordered pore structures of Y-zeolite with an average pore diameter of ca. 1.2 nm were clearly observed over a wide range, while Pd particles could not be recognized on the surface of the zeolite. An electron diffraction analysis also showed no clear diffraction pattern attributable to Pd metal. However, the reduction of $[Pd(NH_3)_4]^{2+}$ on the zeolite surface was confirmed from the results of an XPS analysis. The size of the Pd clusters formed was therefore considered to be less than the diameter of the zeolite pore. The characterization by TEM analysis was found to be very difficult, because the ul-

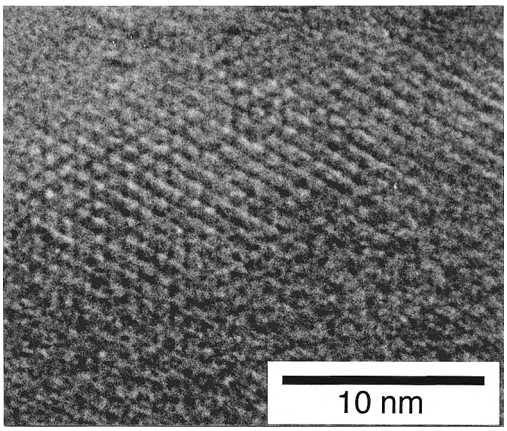

Fig. 6. TEM photograph of the sonochemically prepared Pd–zeolite in the presence of 2-propanol.

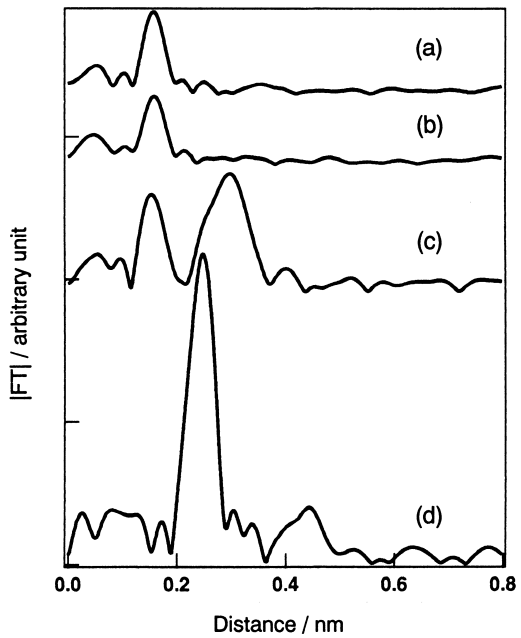

Fig. 7. Radial distribution functions of (a) $Pd(NH_3)_4$–zeolite, (b) irradiated sample of (a), (c) PdO powder, and (d) Pd foil.

trafine Pd particles were located on and inside the insulating zeolite skeleton.

In order to understand the local structures around the Pd atoms and to estimate the size of the Pd clusters, the EXAFS spectra were measured for the samples before and after irradiation.[27] Fourier transforms of the EXAFS spectra are shown in Fig. 7, where the peaks are slightly displaced from the true interatomic distances because of the phase shift, and the filtered ranges of transformation are 30–110 nm^{-1} for a), b), and c) and 29–125 nm^{-1} for d). The results show no distinct peaks due to Pd metal crystals in the Fourier transform of the EXAFS spectrum for the irradiated sample.

An analysis of the X-ray photoelectron spectrum was carried out to obtain further information about the Pd species on the zeolite formed in the sonochemical reduction of $[Pd(NH_3)_4]^{2+}$. Since the X-ray photoelectron spectrum reflects

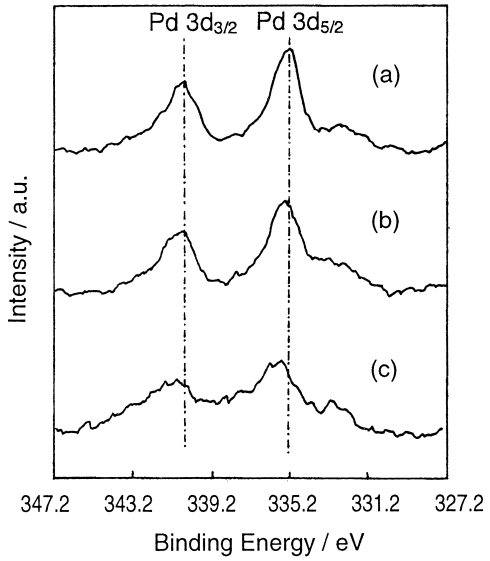

Fig. 8. X-ray photoelectron spectra of Pd 3d core level supported on zeolite samples prepared by conventional gas phase methods. (a) R treatment, (b) O-R1 treatment, (c) O-R2 treatment.

the local electronic states of the observed atoms, a spectral change and a chemical shift of the core level peak should be observed when the electronic states of the Pd atoms changed. For a comparison, Pd-zeolite samples were also prepared by conventional methods [(1) R treatment, (2) O-R1 treatment, and (3) O-R2 treatment],[16] and the relation between the size of the Pd particles and the XPS data was investigated. Figure 8 shows the X-ray photoelectron spectra of the Pd 3d core level of these reference samples. The sample obtained by the R treatment, which is one of the most conventional procedures, had a binding energy of 335.3 eV for the Pd $3d_{5/2}$ core level. It was found that the value for the Pd–zeolite was shifted to a lower energy relative to that of the Pd bulk state (Pd $3d_{5/2}$: 335.95 eV). Mojet et al. reported that the electron density of the Pd particles supported on Na–zeolite is slightly high relative to that of pure Pd, resulting in a shift of the binding energy.[28] Our results could also be explained on the basis of such effects. Because all Pd samples were supported on Y-zeolite in this experiment, this R treatment sample could be regarded as the standard Pd value. It is clearly confirmed in Figure 8 that both peaks of the samples with O-R1 and O-R2 treatments were shifted and broadened more remarkably compared to that with the R treatment.

The data obtained by the EXAFS and XPS measurements are summarized in Table 1, where Fourier transforms (FT) of the EXAFS spectra were carried out to obtain the radial distribution functions. From the Pd–Pd and Pd–N scatterings, the best-fit values of structural parameters were estimated by the inverse FT for each main peak in the FT. In this table, R is the bond distance and N is the average coordination number of the Pd atoms. As references, the data for the unirradiated sample and the standard Pd foil are also given in Table 1. In the radial distribution functions for the unirradiated sample, a predominant peak was observed at $R = 0.208$ nm, which probably corresponds to the Pd–N bond between the Pd^{2+} ions and the ni-

Table 1. Results of EXAFS and XPS Analyses for Pd Species on Zeolite

Samples	EXAFS data			XPS[a]/eV	
	Bond	*R*/nm	*N*	Pd $3d_{3/2}$	Pd $3d_{5/2}$
$Pd(NH_3)_4$–Zeolite	Pd–N	0.208	5.9	344.08	339.03
Pd foil (or black)	Pd–Pd	0.275	12.0	341.18	335.95
R treatment				340.65	335.27
O-R1 treatment	Pd–Pd	0.275	9.6	340.71	335.41
O-R2 treatment	Pd–Pd	0.275	6.8	343.10	335.87
Sonochemically prepared	—[b]	—[b]	—[b]	342.62	336.87

a) Charge-up was corrected with binding energy of C ls. b) No Pd–Pd bond was observed.

trogen atoms in the amine ligands. The *R* of the Pd–Pd bonds in the Pd-zeolite was independent of the processes of the oxidation–reduction treatments, and was equal to that in an infinite Pd crystal. On the other hand, the *N* of the Pd atoms decreased due to these treatments from 9.6 to 6.8, the values of which are much smaller than that in a Pd foil ($N = 12.0$). The discrepancy between these values is attributed mainly to the difference in size of the Pd particles, i. e., *N* in small particles is smaller than that in large crystals because of the high proportion of surface atoms. The sizes of the clusters were estimated using the coordination number for the magic Pd clusters, which are known to be stable clusters with a polyhedron structure. In the case of Pd metal, the atoms are packed in a face-centered cubic structure, and the magic number is reported to be 13 (1-shell), 55 (2-shell), 147 (3-shell), 309 (4-shell) and 561 (5-shell).[29] The average of the coordination numbers (*N*) in the magic clusters can be calculated to be 5.5, 8.0, 8.9, 9.6 and 10.0, respectively. In comparison with the *N* values obtained in the present EXAFS measurements, the average diameter of Pd clusters with $N = 6.8$ and 9.6 could be roughly estimated to be about 0.6–1.0 nm (between 1- and 2-shell) and 1.8 nm (4-shell), respectively. It is clear that the size of the Pd clusters prepared by the hydrogen reduction processes decreases in the order of (R treatment) $>$ (O-R1 treatment) $>$ (O-R2 treatment).

The X-ray photoelectron spectra were characterized according to the Pd size estimated by the EXAFS analyses. It was found that the binding energy of the Pd 3d core level was shifted to a higher energy and the peak became broadened as the size of the Pd particles decreased. Schierbaum et al.[30] recently reported results obtained by XPS analysis during the course of Pt vapor deposition on a clean TiO_2(110) surface under a vacuum. They found that, in the initial period of the Pt deposition, there was a relation between the vaporization time (presumably affecting the size of Pt particles) and the measured binding energy of the Pt 4f core level, in which small Pt particles below the level of the TEM resolution were formed. According to their report, the peak of Pt 4f was observed to be more broadened and shifted to a higher energy in the earlier stages of Pt deposition. On the other hand, with respect to Pd particles, Vedrine et al.[31] and Shpiro et al.[32] previously reported that the peak position of Pd 3d was independent of the particle size. We therefore speculate that the size of the Pd particles mentioned in their reports would be relatively larger (compared to that of Pt particles), and thus the peak shift was not clearly observed.

It was confirmed in the present experiments that the peaks of the Pd 3d core level shifted to a higher energy and broadened with a decrease in the particle size. This result was in good agreement with the tendency for Pt reported by Schierbaum et al., as mentioned above. Therefore, we assumed that the peak shift can be attributed to the quantum size effect of the Pd clusters. Xu et al.[33] recently revealed, furthermore, that a metal-to-nonmetal transition, i.e., a change in the electronic conductivity, occurred in the case of Pd clusters on TiO_2, when the Pd clusters consisted of less than ca. 300 atoms. This transition appears more distinctly with smaller Pd cluster sizes. Thus, the peak shifts of the Pd 3d core level in the present X-ray photoelectron spectra might be explained by the appearance of the quantum size effect. This shift is presumably due to the fact that electrons in the core level are strongly restricted by the atomic nucleus of Pd.[34]

The results from the present study suggest that the formation of metal clusters can be confirmed by the degree of the peak shift in the X-ray photoelectron spectrum. A spectral analysis of the sonochemically prepared Pd-zeolite indicates that the average size of the Pd clusters on the zeolite surface is roughly estimated to be less than 1nm and composed of several dozen Pd atoms. It was suggested that the characterization of the Pd clusters could be qualitatively performed by XPS analyses by considering the quantum size effect. The sonochemical reduction process appears to be a promising method for preparing metal clusters, because radical reactions in a bulk solution proceed at lower temperatures. Further improvements, such as choosing more active organic additives, easily-reducible metal precursors, and supports with a larger pore size, would be necessary for preparing various functional materials.

References

1 W. P. Halperin, *Rev. Mod. Phys.*, **58**, 533 (1986).

2 T. Castro, R. Reifenberger, E. Choi, and R. P. Andres, *Phys. Rev. B*, **42**, 8548 (1990).

3 Y. Volokitin, J. Sinzig, L. J. Dejong, G. Schimd, M. N. Vargaftik, and I. I. Moiseev, *Nature*, **384**, 621 (1996).

4 K. Kimura, and S. Bandow, *Phys. Rev. B*, **37**, 4473 (1988).

5 M. Valden, X. Lai, and D. W. Goodman, *Science*, **281**, 1647 (1998).

6 a) H. Matsumoto and S. Tanabe, *J. Phys. Chem.*, **94**, 4207 (1990). b) H. Matsumoto, S. Tanabe, *J. Mater. Sci. Lett.*, **11**, 623 (1992).

7 a) K. Okitsu, Y. Mizukoshi, H. Bandow, T. A. Yamamoto, Y. Nagata, and Y. Maeda, *J. Phys. Chem. B*, **101**, 5470 (1997). b)

Y. Mizukoshi, K. Okitsu, T. A. Yamamoto, R. Oshima, Y. Nagata, and Y. Maeda, *J. Phys. Chem. B*, **101**, 7033 (1997). c) K. Okitsu, S. Nagaoka, S. Tanabe, H. Matsumoto, Y. Mizukoshi, and Y. Nagata, *Chem. Lett*., **1999**, 271.

8 K. Okitsu, M. Murakami, S. Tanabe, and H. Matsumoto, *Chem. Lett*., **2000**, 1336.

9 K. Okitsu, A. Yue, S. Tanabe, and H. Matsumoto, *Chem. Mater*., **12**, 3006 (2000): A cylindrical glass vessel (volume: 190 mL) was used for ultrasonic irradiation, which had a port covered by a silicon rubber septum for gas bubbling or sampling without exposing the sample to air. The bottom of the vessel was planar, 1mm in thickness, and 55 mmϕ in diameter. The vessel was fixed directly on the oscillator. During operation, the rate of H_2O_2 formation in the sonolysis of pure water was estimated by Fricke dosimetry to be ca. 10 μM/min in the Ar atmosphere.

10 K. Okitsu, H. Bandow, Y. Maeda, and Y. Nagata, and *Chem. Mater*., **8**, 315 (1996).

11 K. Okitsu, Y. Mizukoshi, H. Bandow, Y. Maeda, T. Yamamoto, and Y. Nagata, *Ultrason. Sonochem*., **3**, 249 (1996).

12 a) Y. T. Didenko, W. B. McNamara Ⅲ, and K. S. Suslick, *J. Am. Chem. Soc*., **121**, 5817 (1999). b) E. B. Flint and K. S. Suslick, *Science*, **253**, 1397 (1991). c) "Sonochemistry and Sonoluminescence," ed by L. A. Crum, T. J. Mason, J. Reisse, K. S. Suslick, L. A. Curm Kluwer Publishers, Dordrecht, Netherlands (1999).

13 a) K. S. Suslick, T. Hyeon, and M. Fang, *Chem. Mater*., **8**, 2172 (1996). b) M. M. Mdleleni, T. Hyeon, and K. S. Suslick, *J. Am. Chem. Soc*., **120**, 6189 (1998). c) N. A. Dhas, A. Zaban, and A. Gedanken, *Chem. Mater*., **11**, 806 (1999). d) S. Ramesh, Y. Koltypin, R. Prozorov, and A. Gedanken, *Chem. Mater*., **9**, 546 (1997).

14 a) E. Gachard, J. Belloni, and M. A. Subramanian, *J. Mater. Chem*., **6**, 867 (1996). b) M. Arai, K. Usui, and Y. Nishiyama, *J. Chem. Soc., Chem. Commun*., **1993**, 1853.

15 a) K. J. Klabunde and Y. Imizu, *J. Am. Chem. Soc*., **106**, 2721 (1984). b) K. J. Klabunde, and Y. Imizu, *Science*, **224**, 1329 (1984).

16 H. Matsumoto and S. Tanabe, *Anal. Sci*., **7**, 369 (1991).

17 S. N. Reifsnyder, M. M. Otten, and H. H. Lamb, *Catal. Today*, **39**, 317 (1998).

18 K. Tohji, Y. Udagawa, S. Tanabe, and A. Ueno, *J. Am. Chem. Soc*., **106**, 612 (1984).

19 J. A. Creighton and D. G. Eadon, *J. Chem. Soc., Faraday Trans*., **87**, 3881 (1991).

20 Corrections in the absorption spectra were carried out by considering the concentration of $[Pd(NH_3)_4]Cl_2$ remaining in the irradiated solution. The mole absorption coefficient of Cl^- and NH_4^+ ions was significantly small compared with that of $[Pd(NH_3)_4]Cl_2$, so that the corrections for these ions were not performed in the present report.

21 A. Henglein, *Chem. Mater*., **10**, 444 (1998).

22 A. Henglein and M. Giersig, *J. Phys. Chem*., **98**, 6931 (1994).

23 V. Misik and P. Riesz, *Ultrason. Sonochem*., **3**, 173 (1996).

24 Y. Nagata, Y. Watanabe, S. Fujita, T. Dohmaru, and S. Taniguchi, *J. Chem. Soc., Chem. Commun*., **1992**, 1620.

25 The resonance radius (R_0) of bubbles could be calculated with the following equation, $R_0 = (4/3\omega_a)(P_a - P_h)(2/\rho P_a)^{1/2}[1 + (2/3P_h)(P_a - P_h)]^{1/3}$, where ω_a, P_a, P_h, and ρ are the angular frequency, acoustic pressure, external pressure, and liquid density, respectively [E. A. Neppiras, *Phys. Rep*., **61**, 159 (1980).]. For example, the radius could be estimated to be ca. 13 μm with the parameters of 1.256×10^5 sec^{-1} of ω_a and 1000 kg/m^3 of ρ, and the assumed parameters of 1.01325×10^5 Nm^{-2} of P_h and 2.0265×10^5 Nm^{-2} of P_a. In addition, the collapsing time (τ) was estimated to be less than ca. 0.67 μs with the equation $\tau = 0.915R_0\,[\rho/(P_h + P_a)]^{1/2}$ and the same parameters.

26 V. I. Bukhtiyarov, I. P. Prosvirin, and R. I. Kvon, *J. Electron Spectrosc. Relat. Phenom*., **77**, 7 (1996).

27 S. Tanabe, H. Matsumoto, T. Mizushima, K. Okitsu, and Y. Maeda, *Chem. Lett*., **1996**, 327.

28 B. L. Mojet, M. J. Kappers, J. C. Muijsers, J. W. Niemantsverdriet, J. T. Miller, F. S. Modica, and D. C. Koningsberger, *Stud. Surf. Sci. Catal*., **84**, 909 (1994).

29 References are cited in the following paper; T. Teranishi, and M. Miyake, *Chem. Mater*., **10**, 594 (1998).

30 K. D. Schierbaum, S. Fischer, M. C. Trquemada, J. L. de Segvia, E. Roman, and J. A. Maartin-Gago, *Surface Sci*., **345**, 261 (1996).

31 J. C. Vedrine, M. Dufaux, C. Naccache, B. Imelik, *J. Chem. Soc., Faraday Trans. 1*, **74**, 440 (1978).

32 E. S. Shpiro, G. N. Baeva, A. S. Sass, V. A. Shvets, A. B. Fasman, V. B. Kazanskii, and K. M. Minachev, *Kinet. Catal*., **28**, 1236 (1988).

33 C. Xu, X. Lai, G. W. Zajac, and D. W. Goodman, *Phys. Rev. B*, **56**, 13464 (1997).

34 As the size of Pd metal particles decreases, the degenerate band structure is split, resulting in that the electrons in the Pd 3d level are more strongly restricted by the atomic nuclei in comparison with those in Pd bulk metal. This phenomenon brings about the peak shift in the X-ray photoelectron spectrum to a higher binding energy, which is suggested to be the almost same as that observed for the cationic species often reported.